PRE-BOMB RADIOCARBON VARIABILITY INFERRED FROM A KENYAN CORAL RECORD

Nancy S Grumet[1] • Thomas P Guilderson[2] • Robert B Dunbar[3]

ABSTRACT. We report results from AMS radiocarbon measurements ($\Delta^{14}C$) in corals recovered off the coast of Kenya. Bimonthly samples which span the pre-bomb era average –51‰ (±3.7; n=43), when age and Suess effect are corrected, and over the time of interest (1946–1954) do not exhibit any discernible seasonality. Relative to regional pre-bomb $\Delta^{14}C$ values in the western Indian Ocean, our results indicate ^{14}C enrichment off the coast of Kenya. Furthermore, the absence of a distinct subannual $\Delta^{14}C$ signal suggests that open and coastal upwelling is negligible off the coast of Kenya. Unlike pre-bomb values south of the equator near Seychelles and Madagascar, our pre-bomb value are enriched by more than 10‰. The enrichment of pre-bomb Kenyan $\Delta^{14}C$ values relative to sites around Mauritius, northern Madagascar and Seychelles, suggest that the influence of depleted $\Delta^{14}C$ water transported in the SEC is limited to regions south of 3 to 4°S.

INTRODUCTION

The intimate relationship between the Indian Ocean and the atmosphere is revealed in the seasonal reversal of the Indian-Asian monsoons. The monsoons develop primarily as a response to the large thermal gradients between the Asian continent and the Indian Ocean. During the Northern-Hemisphere winter, a high-pressure cell develops over the Asian land mass and contributes to the creation of the Northeast (NE) monsoon; the extremely cold and dry air masses over land force air from the northeast to the southwest and drive surface ocean circulation counter-clockwise in the northern Indian Ocean. In contrast, during the Northern-Hemisphere summer, the Asian land mass becomes very warm and a low-pressure cell develops and forms the Southwest (SW) monsoon. Strong southwesterly flow in the lower troposphere brings substantial amount of moisture to India and releases it as precipitation from June to September.

The influence of the monsoons on the Indian Ocean is seen in the reversals of the surface circulation and in the hydrological conditions of the surface waters to 10–20°S. The northern and equatorial Indian Ocean circulation is especially complex with large seasonal variations and reversals in major current systems. For example, as a response to prevailing southwesterly flow in the lower troposphere during the SW monsoon, a northward flowing Somali Current (SC) is strongly developed as a continuation of the South Equatorial Current (SEC) and East African Coast Current (EACC) (Figure 1a). Recognized as the western boundary current that causes structural readjustment in the baroclinicity down to 1000 m, the SC is responsible for strong upwelling along the northern coasts of Somali and Oman and the development of the Southern Gyre (SG) and Great Whirl (GW) during the SW monsoon (Luther 1999). Surface water flow is predominantly in an eastward direction. In contrast, during the NE monsoon, northeasterly winds develop causing surface waters north of the equator to flow to the west or southwest comprising the North Equatorial Current (NEC) north of the equator and at the equator, south-flowing water off the coast of Somalia together with the northflowing EACC feed the Equatorial Counter Current (ECC), which moves eastward across the Indian Ocean between 0° and 8°S (Figure 1b) (Schott and McCreary 2001).

The complex oceanography in the northern and equatorial Indian Ocean, briefly described above, is responsible for regional differences in the strength and amount of upwelling of subsurface water. As

[1]Department of Geological and Environmental Sciences, Stanford University, Stanford, California 94305 USA.
 Email: ngrumet@leland.stanford.edu.
[2]Center for Accelerator Mass Spectrometry, Lawrence Livermore National Laboratory, Livermore, California 94551.
 Also at the Institute of Marine Sciences, University of California at Santa Cruz, Santa Cruz, California 65064 USA.
[3]Department of Geological and Environmental Sciences, Stanford University, Stanford, California 94305 USA

a result, there is considerable spatial radiocarbon ($\Delta^{14}C$) variability in surface waters of the western Indian Ocean. This is illustrated in the regional deviations in the ^{14}C offset from atmospheric $^{14}CO_2$, referred to as the reservoir effect, of marine calcareous shells from the northern and equatorial Indian Ocean (Dutta et al. 2001; Southon et al. 2002). For example, Southon et al. (2002) illustrate that Arabian Sea upwelling significantly influences the western Indian Ocean pre-bomb $\Delta^{14}C$ signal. The regional mean using Suess-corrected $\Delta^{14}C$ values for the western Arabian Sea (n=8) is $-73 \pm 2.8\%_o$, while waters farther from the upwelling region, such as those in the tropical Indian Ocean (n=11) yield a regional mean of $-66 \pm 2.6\%_o$ (Southon et al. 2002). The distribution of $\Delta^{14}C$ inferred from carbonates can highlight regional differences in oceanographic processes (e.g., Moore et al. 1997).

Oceanographic measurements of $\Delta^{14}C$, such as those conducted by Geochemical Ocean Section Study (GEOSECS), Indian Gaz Ocean (INDIGO), and World Ocean Circulation Experiment (WOCE) programs have been used to construct vertical profiles of $\Delta^{14}C$ and have increased our understanding of intense monsoon driven upwelling that occurs off the coast of Somalia and the Arabian Coast (e.g. Ostlund and Stuiver 1980; Broecker et al. 1985; Bard et al. 1989; Key et al. 1996). While results from these programs have been extremely valuable, the profiles are subject to
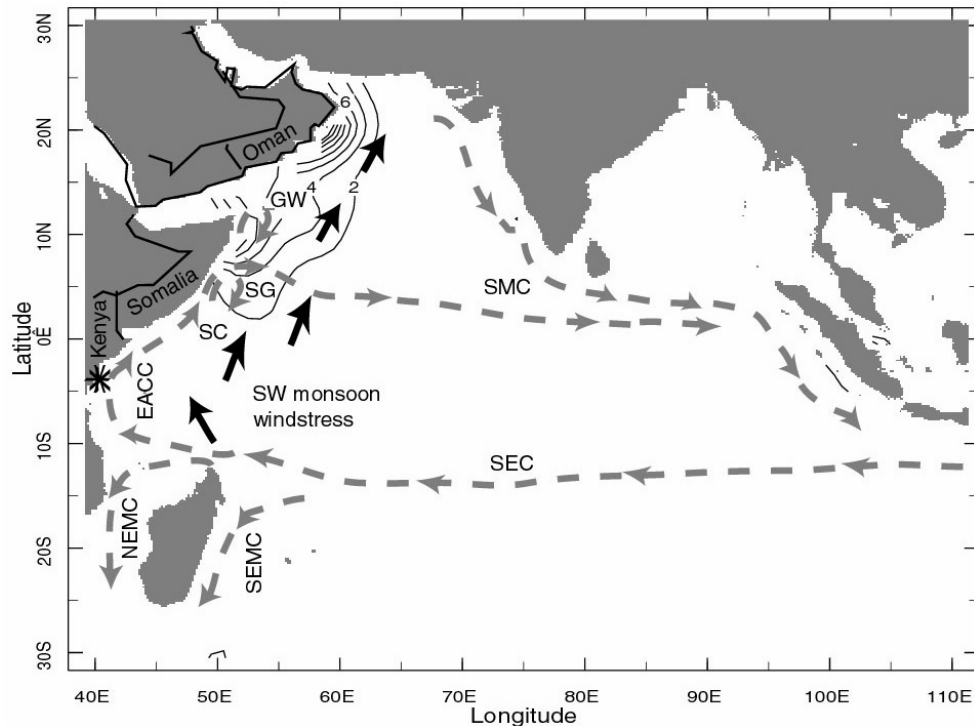

Figure 1a Coral cores were collected by drilling massive colonies of *Porites lutea* off the coast of Kenya, designated by a star, at Malindi (3°14′S, 40°8′E), and Watamu (3°23′S, 39°52′E). Summer (July-Aug.-Sept.) surface (<10 m) nitrate concentrations are shown by contours intervals in μmol/L (Conkright et al. 1998). Surface currents in the Indian Ocean during the SW monsoon: Somali Current (SC), East African Coast Current (EACC), Southwest Monsoon Current (SMC), South Equatorial Current (SEC), and Northeast and Southeast Madagascar Currents (NEMC and SEMC). Upwelling regions are associated with the Southern Gyre (SG) and Great Whirl (GW) (after Schott and McCreary 2001). Thick black arrows indicate predominant SW monsoon wind stress from the US National Centers for Environmental Prediction (NCEP) climatology for July.

temporal aliasing since the measurements represent a "snapshot" of conditions. Such snapshots may be augmented with time series developed from Δ^{14}C record from tropical corals.

^{14}C measurements from banded corals have been shown to represent Δ^{14}C levels of dissolved inorganic carbon (DIC) from the surrounding surface water (Druffel and Linick 1978; Druffel 1982). The accreted aragonite thus provides an unaltered record of ^{14}C/^{12}C ratios present in seawater (e.g. Druffel 1989; Brown et al. 1993; Guilderson et al. 1998; Guilderson et al. 2000). In this study we present the first continuous, bimonthly resolved time series of pre-bomb Δ^{14}C measured in a coral from the western Indian Ocean. These results expand our knowledge of spatial resolution of ^{14}C reservoir corrections in the western Indian Ocean and add a time domain component to this valuable data set. Furthermore, the bimonthly sample resolution allows us to address questions regarding Δ^{14}C variability attributed to the seasonally reversing monsoons. Ultimately, these combined efforts will aid in our understanding of regional oceanography as well as air-sea exchange rates in the Indian Ocean.
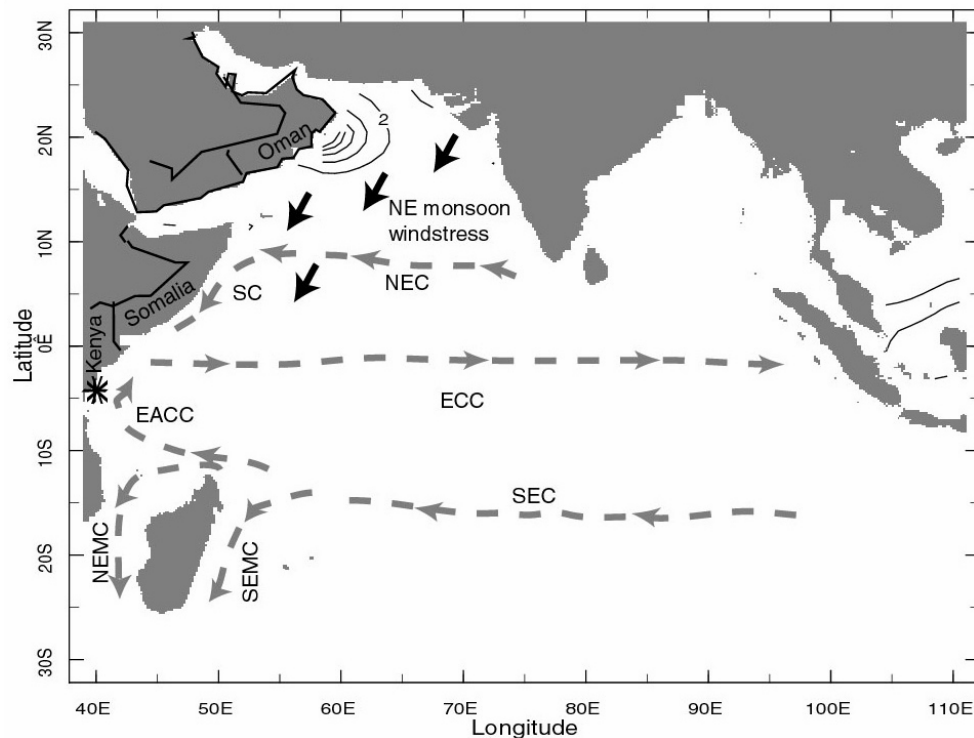

Figure 1b Coral cores were collected by drilling massive colonies of *Porites lutea* off the coast of Kenya, designated by a star, at Malindi (3°14′S, 40°8′E), and Watamu (3°23′S, 39°52′E). Winter (Jan.-Feb.-March) surface (<10 m) nitrate concentrations are shown by contours intervals in µmol/L (Conkright et al. 1998). Surface currents in the Indian Ocean during the NE monsoon: Somali Current (SC), East African Coast Current (EACC), North Equatorial Current (NEC), Equatorial Counter Current (ECC), South Equatorial Current (SEC), and Northeast and Southeast Madagascar Currents (NEMC and SEMC) (after Schott and McCreary, 2001). Thick black arrows indicate predominant NE monsoon wind stress from the US National Centers for Environmental Prediction (NCEP) climatology for January.

METHODS

Cores collected from massive hermatypic corals *Porites lutea* off the coast of Kenya were sampled to assess the seasonal and spatial variability in the coral oxygen isotope ($\delta^{18}O$) and $\Delta^{14}C$ signal (Figure 1a). Coral cores presented here were collected in 1996 from Kenya at Malindi (3°14′S, 40°8′E), and Watamu (3°23′S, 39°52′E). The Malindi coral site is approximately 1 km offshore and at a depth of about 5 m at mean tide. It is an open coast patch reef site on a point. The Watamu coral is approximately 600 m offshore and 200 m landward of an intermittent barrier system. Water depth is about 7 m at the Watamu site. X-radiography of the cores reveals pronounced annual variations in skeletal density and growth rates range from 11 to 15 mm/yr. A transect was mapped along a prominent growth axis of the cores and sampled continuously from the top of the coral slab to approximately 626 mm in the Watamu core and between 325–375 mm in the Malindi core. Samples were collected using a low speed drill to extract aragonite powder every 2 mm for $\Delta^{14}C$ analysis (~6 samples per year) and 1 mm for $\delta^{18}O$ analysis (~12 samples per year).

Oxygen and carbon isotope measurements were analyzed at the Stanford University Stable Isotope Laboratory. Aliquots of coralline aragonite weighing 55 to 95 µg were acidified with orthophosphoric acid at 70 °C and analyzed using a Kiel III carbonate device coupled to a Finnigan MAT 252 mass spectrometer. Approximately 15% of the samples were replicated, yielding an average standard deviation of less than 0.05‰ for $\delta^{18}O$ and 0.12‰ for $\delta^{13}C$. Unknowns were calibrated against a known standard NBS-19 (NIST SRM 8544) and with a Stanford in-house standard (SLS-#1). All results are reported relative to the international V-PDB (Vienna Pee Dee Belemite) standard (Grumet et al. 2001).

Aragonite splits ~10 mg were hydrolyzed to CO_2 in individual reaction chambers, evacuated, heated and acidified with orthophosphoric acid at 90 °C. The resultant CO_2 was converted to graphite in the presence of iron catalyst (Vogel et al. 1987). Graphite targets were measured at the Center for Accelerator Mass Spectrometry (CAMS) facility at Lawrence Livermore National Laboratory (LLNL) (Davis et al. 1990). ^{14}C results are reported as $\Delta^{14}C$ ‰ as defined by Stuiver and Polach (1977). These results include a minor background correction using a calcite standard and are $\delta^{13}C$ and age corrected (Table 1). Concurrent analysis of an in-house standard yielded an external error of ±3.7‰ (1σ, normalized to Fmodern=1.0; n=23).

Well-developed annual density bands and minimum and maximum $\delta^{18}O$ values, as well as a calibration period from 1990–1996, were used to define the chronology parallel to instrumental sea-surface temperature (SST) measurements (Grumet et al. 2001). Instrumental SST records indicate that the maximum (minimum) temperature off the coast of Kenya occurs in March/April (July/August). Accordingly, the minimum and maximum coral $\delta^{18}O$ values were assigned the corresponding calendar date. Samples in between these points were linearly interpolated to make an age model. The assigned calendar months also show a strong correspondence to changes in density. The minimum $\delta^{18}O$ values in April occur within the high-density bands, where calcification exceeds extension when the temperature is the warmest.

RESULTS

In our record, we sample the pre-bomb interval between 1947–1954 (n=43). The pre-bomb record suggests that a fossil fuel correction, known as the Suess Effect, of 14‰ be applied to the age corrected data. This correction is based on back-casting the slope (−0.23‰ yr^{-1}) of the pre-bomb age-corrected data to 1890. However, work by Stuiver and Quay (1981) suggests that the slope of the fossil fuel effect is not constant between 1860–1950, primarily as a result of cosmic ray flux changes.

Table 1 AMS $\Delta^{14}C$ measurements of ~bimonthly Kenyan samples

Coral ID and depth (mm)	Year	CAMS#	$\Delta^{14}C$ [‰] age corrected	±	$\Delta^{14}C$ [‰] Suess corrected[a]
Watamu 96-534	1955	73533	−625	26	−511
Watamu 96-536	1954	73534	−617	26	−508
Watamu 96-538	1954	73535	−581	27	−472
Watamu 96-540	1954	73673	−550	27	−442
Watamu 96-544	1954	73674	−597	28	−490
Watamu 96-546	1954	73675	−630	27	−523
Watamu 96-550	1953	73676	−629	28	−522
Watamu 96-552	1953	73677	−605	27	−498
Watamu 96-554	1953	73678	−624	27	−518
Watamu 96-556	1953	73679	−644	24	−538
Watamu 96-560	1952	73680	−624	29	−519
Watamu 96-562	1952	67915	−658	27	−553
Watamu 96-564	1952	67916	−642	27	−537
Watamu 96-566	1952	67917	−634	27	−530
Watamu 96-568	1952	67918	−617	33	−513
Watamu 96-570	1952	67919	−674	27	−570
Watamu 96-572	1952	67920	−588	27	−484
Watamu 96-574	1951	67921	−567	27	−464
Watamu 96-576	1951	67922	−590	27	−487
Watamu 96-578	1951	67923	−557	27	−454
Watamu 96-582	1951	67924	−644	26	−542
Watamu 96-584	1951	67925	−659	27	−557
Watamu 96-586	1950	67926	−670	27	−569
Watamu 96-588	1950	67927	−633	27	−532
Watamu 96-590	1950	67928	−612	30	−510
Watamu 96-592	1950	67929	−634	25	−533
Watamu 96-594	1950	67930	−605	28	−505
Watamu 96-596	1950	67931	−644	28	−544
Watamu 96-598	1950	67932	−647	35	−547
Watamu 96-600	1949	67933	−676	27	−576
Watamu 96-602	1949	67934	−573	30	−474
Watamu 96-604	1949	67935	−630	28	−531
Watamu 96-606	1949	67936	−620	31	−521
Watamu 96-608	1949	67937	−570	28	−471
Watamu 96-610	1949	67938	−597	28	−499
Watamu 96-612	1948	67939	−559	29	−461
Watamu 96-614	1948	67940	−580	24	−482
Watamu 96-616	1948	67941	−551	28	−453
Watamu 96-618	1948	67942	−471	28	−374
Watamu 96-620	1948	67943	−543	28	−447
Watamu 96-622	1947	67944	−631	28	−535
Watamu 96-624	1947	74050	−681	29	−585
Watamu 96-626	1947	74051	−664	31	−568
Mal96 D2-325	1953	77066	−585	22	−474

Table 1 AMS $\Delta^{14}C$ measurements of ~bimonthly Kenyan samples (*Continued*)

Coral ID and depth (mm)	Year	CAMS#	$\Delta^{14}C$ [‰] age corrected	±	$\Delta^{14}C$ [‰] Suess corrected[a]
Mal96 D2-327	1953	77067	−627	27	−516
Mal96 D2-330	1952	77068	−612	27	−502
Mal96 D2-333	1952	77069	−654	27	−544
Mal96 D2-335	1952	77070	−602	27	−492
Mal96 D2-3375	1952	77071	−653	32	−544
Mal96 D2-340	1952	77072	−596	27	−486
Mal96 D2-341	1952	77073	−671	26	−562
Mal96 D2-3435	1952	77074	−572	24	−463
Mal96 D2-347	1952	77075	−621	34	−513
Mal96 D2-349	1952	77076	−644	26	−535
Mal96 D2-351	1951	77077	−688	25	−580
Mal96 D2-354	1951	77078	−672	32	−564
Mal96 D2-3565	1951	77079	−719	26	−612
Mal96 D2-3595	1951	77080	−647	30	−539
Mal96 D2-3625	1951	77081	−696	26	−589
Mal96 D2-365	1951	77082	−682	31	−575
Mal96 D2-3675	1951	77083	−712	26	−605
Mal96 D2-370	1950	77084	−720	26	−614
Mal96 D2-3725	1950	77085	−681	20	−574
Mal96 D2-375	1950	77086	−664	31	−558

[a]Estimated marine fossil fuel (Suess) effect, 10‰ (1890–1950)

For example, a change in atmospheric ^{14}C trend occurs around 1937 when the gradient changed from −2.8‰ to −6.8‰. Given our limited data set, our back-casted slope most likely overestimates the Suess Effect. Furthermore, the short data set (7 years) can not capture changes associated with dynamic processes operating on an interannual to decadal time scale that are unrelated to the Suess effect. Therefore, we must look to model results and existing pre-bomb coral $\Delta^{14}C$ time series from other sites in order to make an appropriate Suess correction.

The Suess Effect for the central gyres is 7–12‰ according to box diffusion models of Stuiver et al. (1986) and Oeschger et al. (1975). Druffel et al. (2001) measured a value of 7‰ at Hawaii and a range between 10–12‰ for the Florida Keys (Druffel, 1997). Southon et al. (2002) made a fossil fuel correction in the Indian Ocean of 10‰ (1910–1952) by combining model results from Stuiver et al. (1986) and pre-bomb coral samples (Druffel and Suess 1986). We believe a Suess correction of 10‰ is appropriate for the Watamu site given that waters reaching Watamu are relatively shallow (J Southon, personal communication; ERM Druffel, personal communication). All results reported below are age corrected as well as fossil fuel corrected.

Pre-bomb $\Delta^{14}C$ levels measured in the Watamu coral have a range between –58‰ in boreal summer of 1947 to a maximum value of –37‰ in boreal winter of 1948 (Figure 2a). Within the eight-year record, $\Delta^{14}C$ levels average –51‰ with a standard deviation of ±4‰. The average annual range is 6‰, calculated as the difference between the minimum and maximum $\Delta^{14}C$ value within a given year. In order to substantiate our findings from Watamu, we sampled a coral recovered nearby from Malindi. Between 1950 and 1953, Malindi $\Delta^{14}C$ levels have a range between –61‰ in the fall of 1950 to –46‰ in the winter of 1952 (Figure 2b). The average Malindi $\Delta^{14}C$ value is −54‰ with a standard deviation of ±4‰. The average annual range is 7‰.
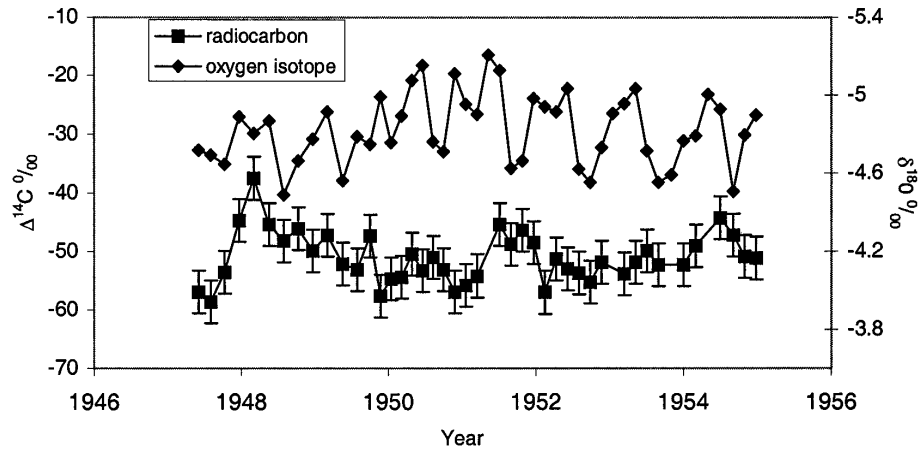
Figure 2a Radiocarbon and oxygen isotope time series from Watamu between 1947 and 1955. Pre-bomb $\Delta^{14}C$ levels measured in the Watamu coral have an annual range between –58‰ in boreal summer of 1947 to a maximum value of –37‰ in boreal winter of 1948. Radiocarbon levels average –51‰ with an average subannual range of 6‰.
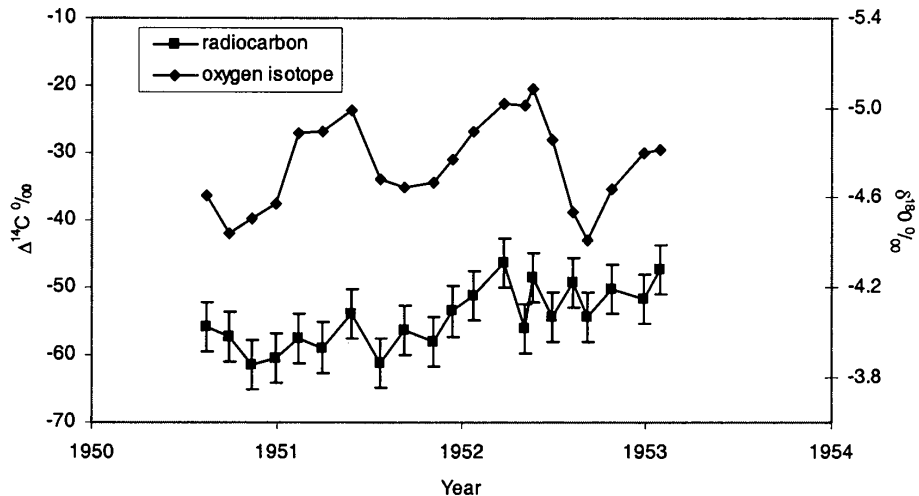

Figure 2b Radiocarbon time series from Malindi between 1950 and 1953. Between 1950 and 1953, Malindi $\Delta^{14}C$ levels have an annual range between –61‰ in the fall of 1950 to –46‰ in the winter of 1952. The average Malindi $\Delta^{14}C$ value is 54 ‰ with an average subannual range of 7‰.

DISCUSSION

The lack of a pronounced seasonal signal distinguishable from the analytical error in the Watamu and Malindi pre-bomb $\Delta^{14}C$ records is consistent with the absence of local upwelling, either due to Ekman pumping driven by strong positive windstress curl or offshore deflection of surface waters by Ekman transport. These results are consistent by nutrient profiles. Profiles from GEOSECS (Spencer et al. 1982) in 1978 and WOCE (R Key, personal communication) in 1995 illustrate a relatively shallow thermocline but nutrient poor surface waters. Average phosphate concentrations in the surface waters (<10 m) off the coast of Kenya from annual LEVITUS94 data (Levitus et al. 1994) are

0.18 μmol/kg and nitrate concentrations are 0.15 μmol/kg. In the upwelling regions of the Arabian Sea nutrient concentrations in the inshore coastal zone are elevated (nitrate is 18 μmol/kg, phosphate is 1.48 μmol/kg) (Woodward et al. 1999). Off the coast of Somalia, in the Great Whirl, nitrate concentration varies between 3 and 8 μmol/kg (Veldhuis et al. 1997). The effect of upwelling is to deliver nutrients and relatively depleted $\Delta^{14}C$ to the upper water column, as observed off the coasts of Somalia and Oman. In contrast, reduced nutrient surface concentrations off the coast of Kenya and concurrent enrichment of $\Delta^{14}C$ characterize the lack of coastal and nearby open-ocean upwelling in this region.

The lack of upwelling off the coast of Kenya is in stark contrast to the productive, vigorous upwelling regions north of the equator. As discussed earlier, the northward flowing Somali Current is responsible for upwelling along the northern coasts of Somali and Oman during the SW monsoon (Luther 1999). As a result, nutrient rich, depleted $\Delta^{14}C$ water strongly influences this region. Southon et al. (2002) estimate a regional $\Delta^{14}C$ mean of –73 ± 2.8‰ in the western Arabian Sea. In contrast, they calculated a mean of –66 ± 2.6‰ in the tropical southwestern Indian Ocean. Combining our results with previous work (Dutta et al. 2001; Southon et al. 2002), there is considerable spatial variability in pre-bomb $\Delta^{14}C$ values in calcareous shells and corals from the western and northern Indian Ocean In many cases, the variability is due to differences in regional ocean circulation patterns discussed above.

Southon et al. (2002) suggest that the influence of monsoon-driven upwelling is propagated throughout the western Indian Ocean by the major current systems, especially the SEC. Relatively depleted $\Delta^{14}C$ values from Sri Lanka (Ceylon) are consistent with this southeast transport of ^{14}C-depleted Arabian Sea water (Southon et al. 2002). Eventually acting as a westward return flow, areas situated in the SEC pathway, such as Mauritius, northern Madagascar and Seychelles exhibit depleted pre-bomb $\Delta^{14}C$ values. Southon et al. (2002) suggest that these values represent advection of ^{14}C-depleted water into the SEC via southeasterly flow from the Arabian Sea. In contrast, our results from the western, equatorial Indian Ocean average –51‰. These samples are enriched by more than 10‰ compared to average southwestern Indian Ocean values reported by Southon et al. (2002). The influence of freshwater could raise the seawater $\Delta^{14}C$ by either equilibrating with atmospheric CO_2 or by increasing the stratification and reducing the amount of vertical mixing. However, the influence of freshwater at Watamu is negligible since the Mida Creek, which is near the coral site, is an ancient creek (McClanahan, personal communication). Furthermore, salinity values range between 33.5 and 36.6 ppt (Obura 1995). These observations suggest that the Watamu site is fairly protected from riverine influence. If the SEC is a source of depleted $\Delta^{14}C$, as Southon et al. (2002) propose, the northern limit of the SEC, and hence the influence of subsurface Indian Ocean water, is apparently south of our sites (3–4°S). This enrichment therefore, suggests that westward return flow of water transported southeast from the Arabian Sea does not reach the surface waters surrounding the Kenyan coral sites, or alternatively there exist spatial-temporal biases in the discrete $\Delta^{14}C$ measurements available.

CONCLUSION

Bimonthly Watamu coral $\Delta^{14}C$ values between 1947 and 1955 averages –51‰. In comparison, surface water pre-bomb $\Delta^{14}C$ levels in the northern Indian Ocean are closer to −73‰ (Southon et al. 2002). Our results demonstrate that there is no immediate source of subsurface, $\Delta^{14}C$ depleted water to the surface water off the coast of Kenya. Surface water nutrient concentrations are consistent with the lack of deeper water replenishment by upwelling in this region. The absence of a distinct subannual $\Delta^{14}C$ signal suggests that coastal and nearby open-ocean upwelling are negligible. Furthermore, the enrichment of pre-bomb Kenyan $\Delta^{14}C$ values relative to sites around Mauritius, northern Mada-

gascar and Seychelles, suggest that the influence of depleted $\Delta^{14}C$ water transported in the SEC is limited to regions south of 3 to 4°S.

ACKNOWLEDGMENTS

REFERENCES

Bard E, Arnold M, Ostlund HG, Maurice P, Monfray P, Duplessy J-C. 1989. Penetration of bomb radiocarbon in the tropical Indian Ocean measured by means of accelerator mass spectrometry. *Earth and Planetary Science Letters* 87:379–89.

Broecker, WS, Peng T-S, Ostlund HG, Stuiver M. 1985. The distribution of bomb radiocarbon in the ocean. *Journal of Geophysical Research* 90:6953–70.

Brown TA, Farwell GW, Grootes PW, Schmidt FH, Stuiver M. 1993. Intra-annual variability of the radiocarbon content of corals from the Galapagos Islands. *Radiocarbon* 35(2):245–51.

Conkright M, Levitus S, O'Brien T, Boyer T, Antonov J, Stephens C. 1998. *World Ocean Atlas 1998 CD-ROM Data Set Documentation.* Technical Report 15. NODC Internal Report, Silver Springs, Maryland. 16 p.

Davis JC, Proctor ID, Southon JR, Caffee MW, Heikkinen DW, Roberts ML, Moore TL, Turteltaub KW, Nelson DE, Loyd DH, Vogel JS. 1990. LLNL/UC AMS facility and research program Nuclear. *Instruments and Methods in Physics Research B* 52:269–72.

Druffel EM, Linick TW. 1978. Radiocarbon in annual coral rings of Florida. *Geophysical Research Letters* 5:913–6.

Druffel EM, Suess HE. 1983. On the radiocarbon record in banded corals: exchange parameters and net transport of the $^{14}CO_2$ between atmosphere and surface ocean. *Journal of Geophysical Research* 88:1271–80.

Druffel EM. 1982. Banded corals: changes in oceanic ^{14}C during the Little Ice Age. *Science* 218:13-9.

Druffel ERM. 1989. Decade time scale variability of ventilation in the North Atlantic: high precision measurements of bomb in banded corals. *Journal of Geophysical Research* 94:3271–85.

Druffel ERM. 1997. Geochemistry of corals: Proxies of past ocean chemistry, ocean circulation, and climate. *Proceedings of National Academy of Science* 94: 8354–61.

Druffel ERM, Griffin S, Guilderson TP, Kashgarian M,

Southon J, Schrag DP. 2001. Changes in subtropical North Pacific radiocarbon and correlation with climate variability. *Radiocarbon* 43(1):15–25.

Dutta K, Bhushan R, Somayajulu BLK. 2001. ΔR correction values for the northern Indian Ocean. *Radiocarbon* 43(2A):483–8.

Grumet NS, Dunbar RB, Cole JE. 2001. Multisite record of climate change from Indian Ocean corals. *9th International Coral Reef Symposium*, Bali, Indonesia. Forthcoming.

Guilderson TP, Schrag DP, Kashgarian M, Southon J. 1998. Radiocarbon variability in the western equatorial Pacific inferred from a high-resolution coral record from Nauru Island. *Journal of Geophysical Research* 103:24,641–50.

Guilderson TP, Schrag DP, Goddard E, Kashgarian M, Wellington GM, Linsley BK. 2000. Southwest subtropical Pacific surface water in a high-resolution coral record. *Radiocarbon* 42(2):249–56.

Key RM, Quay PD, Jones GA, McNichol AP, von Reden KF, Schneider R. 1996. WOCE AMS radiocarbon 1 Pacific Ocean results P6, P16 and P17. *Radiocarbon* 38(3):425–518.

Levitus S, Burgett R, Boyer T. 1994. *World ocean atlas 1994. Volume 3: nutrients.* Washington DC: NOAA Atlas NESDIS 3, US Department of Commerce.

Luther ME. 1999. Interannual variability in the Somali Current 1954-1976. *Nonlinear Analysis* 35:59–83.

Moore MD, Schrag DP, Kashgarian M. 1997. Coral constraints on the source of the Indonesian throughflow. *Journal of Geophysical Research* 102:12,359–65.

Obura D. 1995. Environmental stress and life history strategies, a case study of corals and river sediment from Malindi, Kenya. PhD dissertation. University of Miami.

Oeschger H, Siegenthaler U, Schotterer U, Gugelmann A. 1975. Box diffusion-model to study carbon-dioxide exchange in nature. *Tellus* 27:168–92.

Ostuland HG, Stuiver M. 1980. GEOSECS Pacific radio-

carbon. *Radiocarbon* 22(1):25–53.

Schott FA, McCreary JP. 2001. The monsoon circulation of the Indian Ocean. *Progress in Ocean.* 51:1–123.

Southon J, Kashgarian M, Fontugne M, Metivier B, Yim WWS. 2002. Marine reservoir corrections for the Indian Ocean and Southeast Asia. *Radiocarbon* 44(1): 167–80.

Spencer D, Broecker WS, Craig H, Weiss RF. 1982. *Geosecs Indian Ocean Expedition. Volume 6, Sections and Profiles IDOE.* National Science Foundation. 140 p.

Stuiver M, Polach HA. 1977. Discussion reporting of ^{14}C data. *Radiocarbon* 19(3):355–63.

Stuiver M, Quay PD. 1981. Atmospheric ^{14}C changes resulting from fossil fuel CO_2 release and cosmic ray flux variability. *Earth and Planetary Science Letters* 53:349–362.

Stuiver M, Pearson GW, Braziunas TF.1986. Radiocarbon age calibration of marine samples back to 9000 cal BP. *Radiocarbon* 28(2B):980–1021.

Swallow JC. 1984. Some aspects of the physical oceanography of the Indian Ocean. *Deep-Sea Research* 31: 639–50.

Tomczak M, Godfrey, JS. 1994. *Regional oceanography: an introduction*. Oxford: Pergamon Press. 422 p.

Veldhuis MJW, Kraay GW, Van Bleijswijk GD, Baars MA. 1997. Seasonal and spatial variability in phytoplankton biomass, productivity and growth in the northwestern Indian Ocean: the southwest and northeast monsoon, 1992–1993. *Deep-Sea Research I* 44: 425–49.

Vogel JS, Southon JR, Nelson DE. 1987. Catalyst and binder effects in the use of filamentous graphite for AMS. *Nuclear Instruments and Methods in Physics Research B* 29:50–6.

Woodward EMS, Rees AP, Stephens JA. 1999. The influence of the southwest monsoon upon the nutrient biogeochemistry of the Arabian Sea. *Deep-Sea Research II* 46:571–91.